Universiteit Utrecht

Utrecht University

Institute for Theoretical Physics

Bachelor's Thesis

Transverse spin injection: from scattering theory to skyrmions

Author:
Laurens Stronks
3864502

Supervisor:
Dr. Rembert Duine

June 17, 2014

Abstract

In this Thesis we theoretically investigate charge-current-induced spin current injection as a result of a gradient in the magnetization on an interface between a ferromagnetic material and a normal metal, using a continuum scattering method in a three terminal set-up. We find that the injected spin current is determined by the magnetization, its derivative and their cross product. We also find an expression for the reverse effect, a spin-current-induced charge current on the same interface. As an application, we consider the injected spin current due to a charge current flowing through a magnetic skyrmion and the effect it has on the skyrmion dynamics. We find that the speed of the skyrmion can be tuned by adjusting the thickness of the layer of the normal metal.

Contents

1 Introduction

In the field of spintronics, spin currents are of great importance [1]. If these currents, in which electrons with different spin move in different directions, can be controlled and detected, it would for instance be very useful for the development of storage devices that use the spin of an electron. There are multiple ways to induce a spin current, such as the spin Hall effect [2] and the spin Seebeck effect [3].

Recently another method for the injection of a spin current was proposed on the interface of a ferromagnetic and a nonmagnetic metal (FM-NM) [4]. If a charge current $\boldsymbol{j}^c$ flows along such an interface, a spin current is injected into the normal metal, with spin polarization equal to

$$\boldsymbol{j}^s_{in} = -\frac{\hbar g g_L \mu_B P}{8\pi G_0 M_s |e|} \boldsymbol{\Omega}(\boldsymbol{x}) \times [(\boldsymbol{j}^c \cdot \nabla)\boldsymbol{\Omega}(\boldsymbol{x})]. \tag{1}$$

In this equation, g is an interface parameter, g_L is the Landé g factor, μ_B is the Bohr magneton, P is the spin polarization of the spin current in the ferromagnet, G_0 is the quantum of conductance, M_s is the saturation magnetization, e is the electron charge and $\boldsymbol{\Omega}$ is the unit magnetization vector in the ferromagnetic metal. The situation is schematically depicted in Fig. 1.

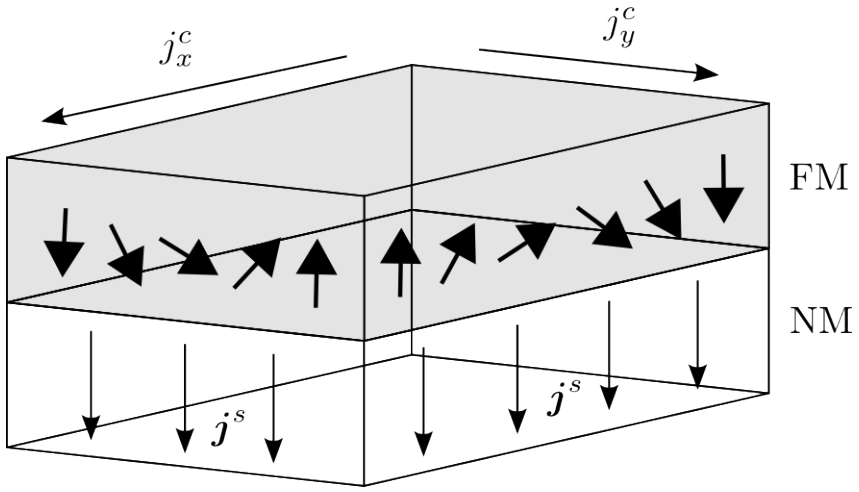

Figure 1: An interface between a ferromagnetic metal (FM) and a normal metal (NM) and a charge current flowing along it. Provided that the gradient of the magnetization is nonzero, a transverse spin current is injected into the normal metal.

It is important to note that this effect requires the magnetization to be nonconstant. Otherwise, the injected spin current would be zero according to Eq. (1). In Chapter 2 of this Thesis, we look at a spin current injection that has terms that scale with the magnetization gradient as well. Instead of using a tight-binding method as in Ref. [4], we use a continuum scattering description with three terminals to find the spin current injection in one of the terminals as a result of a charge current through the other two. We find a similar expression to the one in Eq. (1), where the spin polarization of the injected spin current scales with the cross product of the magnetization and its gradient.

After that we turn to the reverse effect of that in Eq. (1), which is a charge current on the FM-NM interface induced by a spin current in the nonmagnetic metal. This effect suggests an immediate method for detecting a spin current by measuring the induced charge current (or the corresponding voltage difference).

Finally, in Chapter 3 we study an application of the injected spin current, in the form of the dynamics of a skyrmion. Skyrmions are interesting because they could be used in memory devices to carry information [5]. A skyrmion is a configuration of the magnetization that looks like a spiral. In Ref. [6], the dynamics of a skyrmion as a result of a charge current was studied. We will follow the same steps for a skyrmion on a FM-NM interface on which the charge current will also induce a spin current into the normal metal, which in turn leads to an extra torque on the skyrmion. It turns out that the resulting speed of the skyrmion is tunable by varying the thickness of the normal metal layer.

We start the next chapter with a simple model to find an injected spin current using a continuum scattering method. After that, we use time reversal symmetry to simplify the result. Then a more complex situation is studied to find an injected spin current of the same form as in Eq. (1). In Chapter 3 we first find the profile of the skyrmion, after which we study the dynamics of the skyrmion.

2 A current-induced spin current as a result of a gradient in the magnetization

In the first few sections of this chapter we use Landauer-Büttiker theory to find an expression for the spin current. We consider electrons that are scattered on a region with constant magnetization. Assuming we know all the transmission and reflection coefficients we can derive an expression for the spin current in terms of those coefficients. In the last section we look at the reverse effect of Eq. (1), using the theory of Onsager reciprocity.

2.1 The interface parameter g

In Ref. [4] the interface parameter g in Eq. (1) was found by using a tight-binding method. In the following, we will derive an expression for a spin current injection in the normal metal using an alternative method: we assume the electrons are scattered by a magnetic region in space. First, we consider the case with only one such region and the polarization of the spin current will then only have a term which scales with the magnetization $\mathbf{\Omega}$. After that, we turn to a more complex set-up, for which the polarization of the spin current will have more terms, including one containing the cross product of the magnetization and its gradient, just like in Eq. (1).

2.1.1 Scattering on a ferromagnet with constant magnetization

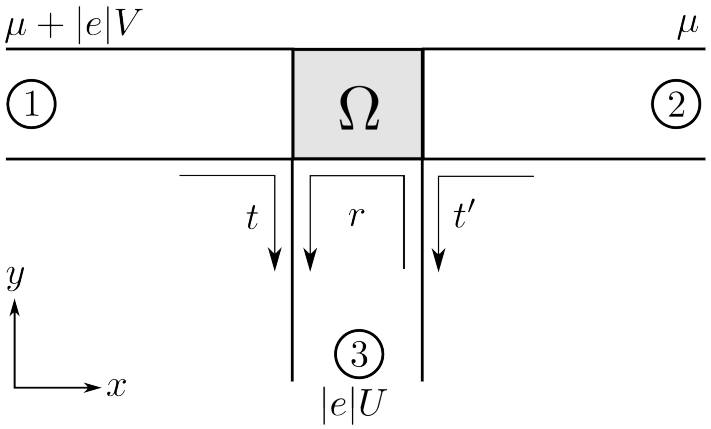

Figure 2: A three-terminal scattering set-up, with all terminals ending in a magnetic element with constant magnetization $\mathbf{\Omega}$, with t and t' the transmission coefficients from terminal 1 and 2 to terminal 3 and r the reflection coefficient in terminal 3.

We first consider the two-dimensional set-up of Fig. 2, which consists of three terminals which all end at a small rectangular magnetic region with constant magnetization $\mathbf{\Omega}$. The goal is to find the spin current in terminal 3 as a result of scattering off the ferromagnetic region. Assuming that the potentials in all terminals are constant and that the terminals are narrow enough to consider them as one-dimensional, we can describe the spatial part of the wave function for an incoming electron in terminal 1 as $\psi(x) = Ae^{ikx}$, with A some normalization constant. For an electron with spin up ($|\uparrow\rangle$) which enters terminal 1 there are multiple possibilities for what will happen. The electron can be reflected or transmitted into either terminal 2 or 3 and the spin of the electron can stay the same or change to spin down ($|\downarrow\rangle$). We are interested in the

resulting spin current in terminal 3. As a result of the spin rotation symmetry, the transmission coefficients for an electron can be written as

$$t = \begin{pmatrix} t_{\uparrow\uparrow} & t_{\downarrow\uparrow} \\ t_{\uparrow\downarrow} & t_{\downarrow\downarrow} \end{pmatrix} = t_s \mathbb{1} + t_t \boldsymbol{\Omega} \cdot \boldsymbol{\tau}. \tag{2}$$

Here, t_{ij} is the reflection coefficient for an incoming electron with spin projection $|i\rangle$ and outgoing with spin projection $|j\rangle$. Furthermore, $\mathbb{1}$ is the 2×2 identity matrix and $\boldsymbol{\tau}$ is a vector containing the Pauli matrices as entries. The coefficients t_s and t_t are complex numbers which are fully determined by transmission in the case $\boldsymbol{\Omega} = \hat{\boldsymbol{z}}$. For a single electron entering terminal 1 with spin ($|\uparrow\rangle$), the wave function in terminal 3 is given by

$$\psi(y) = A e^{-iky} \left(t_{\uparrow\uparrow} |\uparrow\rangle + t_{\uparrow\downarrow} |\downarrow\rangle \right). \tag{3}$$

The spin current $\boldsymbol{I}_1^s$ in the third terminal as a result of this single electron is given by the expectation value of the spin current operator $\frac{\hbar}{2}\boldsymbol{\tau} p$, where $p = -i\hbar\frac{d}{dy}$ is the momentum operator:

$$\boldsymbol{I}^s_{1,1\uparrow} = -\frac{\hbar^2 k}{2m} \left(t^*_{\uparrow\uparrow} \langle\uparrow| + t^*_{\uparrow\downarrow} \langle\downarrow| \right) \boldsymbol{\tau} \left(t_{\uparrow\uparrow} |\uparrow\rangle + t_{\uparrow\downarrow} |\downarrow\rangle \right). \tag{4}$$

To find the total spin current in the terminal as a result of incoming electrons out of terminal 1, we have to take into account the contribution of incoming electrons with spin $|\downarrow\rangle$ and integrate over al possible wave numbers k. The total spin current is given by

$$\boldsymbol{I}^s_{tot,1} = \boldsymbol{\Omega} \int_0^{\mu+|e|V} d\epsilon \left(t_s^* t_t + t_s t_t^* \right). \tag{5}$$

as derived in Appendix A.1 and were zero temperature is assumed. It should be noted that this can be written as the integral over $t_s^* \left(t_t \boldsymbol{\Omega}\right) + t_s \left(t_t \boldsymbol{\Omega}\right)^*$, which will become important in the next example. For the total spin current in terminal 3 we need to sum the contributions from all terminals

$$\boldsymbol{I}^s_{tot} = \boldsymbol{\Omega} \left(\int_0^{\mu+|e|V} d\epsilon \left(t_s^* t_t + t_s t_t^* \right) + \int_0^{\mu} d\epsilon \left(t_s^* t_t + t_s t_t^* \right) + \int_0^{|e|U} d\epsilon \left(r_s^* r_t + r_s r_t^* \right) \right), \tag{6}$$

as is derived in Appendix A.1. Here, r_s and r_t are the coefficients for reflection in terminal 3, defined similarly to Eq. (2). It should be noted that we assume $t = t'$ because of the symmetry of the problem.

There is also another way to look at this problem, using the Landauer formula, which states that the conductance scales with the transmission coefficient. First, we note that $2(t_s^* t_t + t_s t_t^*) = |\tilde{t}_{\uparrow\uparrow}|^2 - |\tilde{t}_{\downarrow\downarrow}|^2$, with $\tilde{t}_{\uparrow\uparrow}$ and $\tilde{t}_{\downarrow\downarrow}$ the transmission coefficients for a spin-$|\uparrow\rangle$ and $|\downarrow\rangle$ electron respectively in the case $\boldsymbol{\Omega} = \hat{\boldsymbol{z}}$. This agrees with the intuitive notion of a spin current that different spins move in different directions. We now set $\boldsymbol{\Omega} = \hat{\boldsymbol{z}}$, so that the system is collinear. In that case we can treat spin up and down separately, because no spin flip takes place according to Eq. (2). The current of spin τ-particles in terminal 3 is given by [7]

$$I_\tau = \frac{|e|}{2\pi} |\tilde{t}_{\tau\tau}|^2 (U - V_1), \tag{7}$$

where V_1 is the potential in terminal 1. Here we used the fact that the transmission coefficients for transmission in the opposite direction are equal, which will be proven in the next section.

The spin current in terminal 3 is given by subtracting the spin-$|\downarrow\rangle$ current from the spin-$|\uparrow\rangle$ and summing the contributions from terminal 1 and 2. Taking into account that the spin polarization vector is in the $\mathbf{\Omega}$ direction, we can write the spin current in terminal 3 as

$$\boldsymbol{I}^s = \frac{|e|\mathbf{\Omega}}{2\pi}(|\tilde{t}_{\uparrow\uparrow}|^2 - |\tilde{t}_{\downarrow\downarrow}|^2)(U - V_1 - V_2). \tag{8}$$

This expression is similar to the one in Eq. (6), but the integral has now been carried out.

2.1.2 Time reversal symmetry and scattering

Before we proceed with the next example of an injected spin current, we make a digression to find a relation between transmission coefficients for transmission in the opposite direction, which we already used in the previous paragraph. A set-up with only two terminals will be used but this theory can easily be extended to more terminals. The situation we will consider is depicted in Fig. 3.

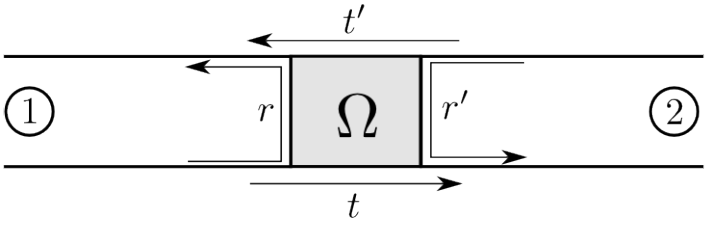

Figure 3: The same set-up as in Fig. 2, but now with only two terminals. The transmission and reflection coefficients from the left are t and r and from the right we have t' and r'.

We will follow the same steps as in Ref. [8]. There, a simple relation is derived for the scattering matrix for a system with time reversal symmetry. However, our system is not invariant under time reversal, since the magnetization $\mathbf{\Omega}$ will change to $-\mathbf{\Omega}$ if $t \to -t$. On the left side, we have a wave function $|\psi\rangle_{L\tau} = \phi^{in}_{L\tau}|\rightarrow \tau\rangle + \phi^{out}_{R\tau}|\leftarrow \tau\rangle$ and on the right side we have $|\psi\rangle_{R\tau} = \phi^{out}_{R\tau}|\rightarrow \tau\rangle + \phi^{in}_{L\tau}|\leftarrow \tau\rangle$. Here, the arrow in the bra gives the direction of the velocity and τ gives the spin projection of the state and can be either up ($\uparrow$) or down ($\downarrow$).

We define the incident wave amplitude as $a = \left(\phi^{in}_{L\uparrow}, \phi^{in}_{L\downarrow}, \phi^{in}_{R\uparrow}, \phi^{in}_{R\downarrow}\right)^T$ and the outgoing wave amplitude is $b = \left(\phi^{out}_{L\uparrow}, \phi^{out}_{L\downarrow}, \phi^{out}_{R\uparrow}, \phi^{out}_{R\downarrow}\right)^T$, where the T denotes the transpose. The 2×2 transmission and reflection matrices for the left side are t and r respectively and for the right side we define t' and r' in a similar fashion. By definition of the scattering matrix $S_{\mathbf{\Omega}}$, we can write

$$b = S_{\mathbf{\Omega}} a \tag{9}$$

where $S_{\mathbf{\Omega}}$ is a 4×4 matrix given by

$$S_{\mathbf{\Omega}} = \begin{pmatrix} r & t' \\ t & r' \end{pmatrix}. \tag{10}$$

Since probability should be conserved, S is unitary. Because of that we can rewrite Eq. (9) as

$$a^* = S^T_{\mathbf{\Omega}} b^*. \tag{11}$$

We now introduce the time reversal operator Θ. For spin $\frac{1}{2}$-particles, such as electrons, Θ can be written as

$$\Theta = -i\tau_y K. \tag{12}$$

Here, K denotes the complex conjugation operator. This operator reverses the direction of the particle, which is clear from the preceding example. Indeed, the spatial part of the wave function was given by e^{ikx} and complex conjugation is equivalent to changing k to $-k$. It should be noted that τ_y is a 2×2 Pauli matrix that works on all transmission and reflection matrices in the scattering matrix separately, so Θ can be understood as [9]

$$\Theta = KC = K \begin{pmatrix} 0 & -1 & 0 & 0 \\ 1 & 0 & 0 & 0 \\ 0 & 0 & 0 & -1 \\ 0 & 0 & 1 & 0 \end{pmatrix}, \tag{13}$$

where C is the 4×4-matrix above.

Just as in Ref. [8], we have $\Theta b = Ca^*$ and $\Theta a = Cb^*$. One finds

$$a^* = -C\Theta b = -C\Theta S_{\mathbf{\Omega}} a = -CS_{-\mathbf{\Omega}}\Theta a = -CS_{-\mathbf{\Omega}} C b^*, \tag{14}$$

where we used Eq. (9) and the fact that $\Theta S_{\mathbf{\Omega}} = S_{-\mathbf{\Omega}}\Theta$, which follows from the fact that time reversal symmetry changes the magnetization from $\mathbf{\Omega}$ to $-\mathbf{\Omega}$. Combining this with Eq. (11) leads to the conclusion

$$S_{\mathbf{\Omega}}^T = -CS_{-\mathbf{\Omega}} C. \tag{15}$$

To profit from this relation, we just plug in Eq. (10) and Eq. (2). Using $t = t_s \mathbb{1} + t_t \mathbf{\Omega} \cdot \boldsymbol{\tau}$, $t' = t'_s \mathbb{1} + t'_t \mathbf{\Omega} \cdot \boldsymbol{\tau}$, $r = r_s \mathbb{1} + r_t \mathbf{\Omega} \cdot \boldsymbol{\tau}$ and $r' = r'_s \mathbb{1} + r'_t \mathbf{\Omega} \cdot \boldsymbol{\tau}$, we find from Eq. (15) that

$$\begin{pmatrix} r_s - r_t\Omega_z & -r_t(\Omega_x + i\Omega_y) & t_s - t_t\Omega_z & -t_t(\Omega_x + i\Omega_y) \\ -r_t(\Omega_x + i\Omega_y) & r_s + r_t\Omega_z & -t_t(\Omega_x + i\Omega_y) & t_s + t_t\Omega_z \\ t'_s - t'_t\Omega_z & -t'_t(\Omega_x + i\Omega_y) & r'_s - r'_t\Omega_z & -r'_t(\Omega_x + i\Omega_y) \\ -t'_t(\Omega_x - i\Omega_y) & t'_s + t'_t\Omega_z & -r'_t(\Omega_x - i\Omega_y) & r'_s + r'_t\Omega_z \end{pmatrix} =$$
$$\begin{pmatrix} r_s - r_t\Omega_z & -r_t(\Omega_x + i\Omega_y) & t'_s - t'_t\Omega_z & -t'_t(\Omega_x + i\Omega_y) \\ -r_t(\Omega_x + i\Omega_y) & r_s + r_t\Omega_z & -t'_t(\Omega_x + i\Omega_y) & t'_s + t'_t\Omega_z \\ t_s - t_t\Omega_z & -t_t(\Omega_x + i\Omega_y) & r'_s - r'_t\Omega_z & -r'_t(\Omega_x + i\Omega_y) \\ -t'_t(\Omega_x - i\Omega_y) & t'_s + t'_t\Omega_z & -r'_t(\Omega_x - i\Omega_y) & r'_s + r'_t\Omega_z \end{pmatrix}. \tag{16}$$

It follows immediately that $t_s = t'_s$ and $t_t = t'_t$, which tells us that the transmission matrices for transmission in the opposite direction are equal. This situation is easily generalized to n terminals. In that case, the relation (15) is the same, but the matrix C will be a $2n \times 2n$-matrix, extended by adding an extra copy of the 2×2-matrix $-i\tau_y$, for each extra terminal, on the diagonal.

2.1.3 A spin current as a result of a gradient in the magnetization

Now, we consider the following situation, depicted in Fig. 4. Now, there are two ferromagnetic regions with slightly different magnetization, $\mathbf{\Omega}_1$ and $\mathbf{\Omega}_2$ respectively. Therefore, $\mathbf{\Omega}_2$ can be approximated by $\mathbf{\Omega}_2 \approx \mathbf{\Omega}_1 + \frac{\partial \mathbf{\Omega}_1}{\partial x} dx$, where dx is the small distance between the two ferromagnetic regions. In principle, there are infinitely many reflections possible between the two ferromagnetic

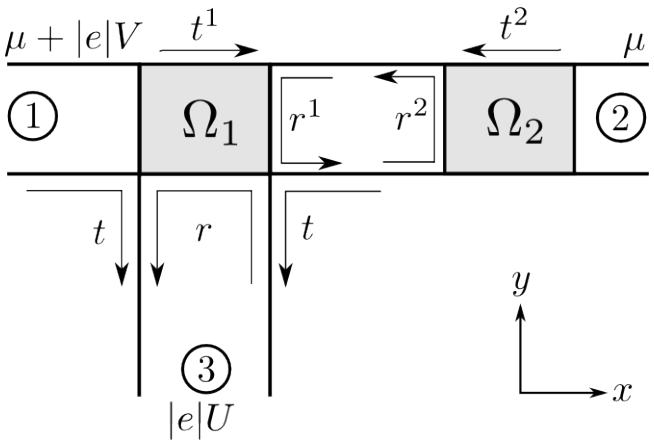

Figure 4: Another three-terminal scattering set-up, now with two magnetic boxes with different magnetizations $\mathbf{\Omega_1}$ and $\mathbf{\Omega_2}$. The transmission and reflection coefficients t, t_1, t_2, r, r_1 and r_2 correspond to the arrows depicted above.

boxes, but only terms that contain at most two reflections will be considered. Again, we are going to sum the contributions of all terminals. First we need to find the transmission matrices and reflection matrices for all relevant situations. Suppose for instance an incident particle in terminal 1. It can either be transmitted directly into terminal 3 or it can take the route tr^2t^1 to enter terminal 3. So, the total transmission coefficient is given by

$$t_{1\to 3} = t + tr^2t^1. \tag{17}$$

Similarly, the transmission coefficient for an electron entering terminal 2 is

$$t_{2\to 3} = t(\mathbb{1} + r^2r^1)t^2, \tag{18}$$

and the reflection coefficient in terminal 3 is

$$t_{3\to 3} = r + tr^2t, \tag{19}$$

where we used the fact that the transmission coefficients for transmission in the opposite direction are equal. The only thing we have to do is to express these matrices in the form

$$t_{i\to 3} = a_i\mathbb{1} + b_i\boldsymbol{v}_i \cdot \boldsymbol{\tau}, \tag{20}$$

with $\boldsymbol{v}_i$ an arbitrary three-dimensional vector and a_i and b_i arbitrary complex numbers. In that case we can use the observation we made at the end of Chapter 2.1.1 that the spin current in terminal 3 as a result of the electrons that enter terminal i is an integral over $a_i(b_i\boldsymbol{v}_i)^* + a_i^*(b_i\boldsymbol{v}_i)$. As it turns out, it is always possible to write the transmission and reflection coefficients in the form of Eq. (20). This follows from the fact that, for arbitrary vectors $\boldsymbol{v}$ and $\boldsymbol{w}$, we have

$$\begin{aligned}(\boldsymbol{v}\cdot\boldsymbol{\tau})(\boldsymbol{w}\cdot\boldsymbol{\tau}) &= v_a\tau_a w_b\tau_b \\ &= (v_a w_b)(\delta_{ab}\mathbb{1} + i\epsilon_{abc}\tau_c) \\ &= (\boldsymbol{v}\cdot\boldsymbol{w})\mathbb{1} + i(\boldsymbol{v}\times\boldsymbol{w})\cdot\tau,\end{aligned} \tag{21}$$

where we used the Einstein summation convention. Expressions for a_i, b_i and $\boldsymbol{v}_i$ are derived in Appendix A.2 and are shown in Tab. 1. It follows that the contribution of each terminal

contains three terms: one that scales with $\mathbf{\Omega}_1$, one that scales with the gradient of $\mathbf{\Omega}_1$ and one scaling with the cross product of the two, i.e. $\mathbf{\Omega}_1 \times \frac{\partial \mathbf{\Omega}_1}{\partial x}$. This last term is of the same form as the spin injection of Eq. (1). Since $\mathbf{\Omega}_1$, $\frac{\partial \mathbf{\Omega}_1}{\partial x}$ and $\mathbf{\Omega}_1 \times \frac{\partial \mathbf{\Omega}_1}{\partial x}$ are orthogonal, they span the whole space which means the spin polarization can in principle be in any direction. However, it should be noted that the coefficients in front of the vectors are completely determined by the transmission and reflection coefficients in the case $\mathbf{\Omega} = \hat{\boldsymbol{z}}$ and the potentials in the three terminals.

a_1	=	$t_s(1 + r_s^2 t_s^1 + r_t^2 t_t^1) + t_t(r_t^2 t_s^1 + r_s^2 t_t^1)$
a_2	=	$t_s((1 + r_s^2 r_s^1 + r_t^2 r_t^1)t_s^2 + (r_s^2 r_t^1 + r_t^2 r_s^1))t_t^2 + t_t((1 + r_s^2 r_s^1 + r_t^2 r_t^1)t_t^2 + (r_s^2 r_t^1 + r_t^2 r_s^1)t_s^2)$
a_3	=	$r_s + t_s(r_s^2 t_s + r_t^2 t_t) + t_t(r_t^2 t_s + r_s^2 t_t)$
$b_1 \boldsymbol{v}_1$	=	$(t_s(1 + r_s^2 t_s^1 + r_t^2 t_t^1) + t_t(r_t^2 t_s^1 + r_s^2 t_t^1))\mathbb{1} + ((t_s(r_t^2 t_s^1 + r_s^2 t_t^1) + t_t(1 + r_s^2 t_s^1 + r_t^2 t_t^1))\mathbf{\Omega}_1 + i(t_s r_t^2 t_t^1 + t_t r_t^2 t_s^1)\mathbf{\Omega}_1 \times \frac{\partial \mathbf{\Omega}_1}{\partial x} dx + (t_s r_t^2 t_s^1 - t_t r_t^2 t_t^1)\frac{\partial \mathbf{\Omega}_1}{\partial x} dx$
$b_2 \boldsymbol{v}_2$	=	$(t_s((1+r_s^2 r_s^1+r_t^2 r_t^1)t_s^2+(r_s^2 r_t^1+r_t^2 r_s^1))t_t^2+t_t((1+r_s^2 r_s^1+r_t^2 r_t^1)t_t^2+(r_s^2 r_t^1+r_t^2 r_s^1)t_s^2))\mathbf{\Omega}_1 + (t_s(r_t^2 r_s^1 t_s^2 + (1 + r_s^2 r_s^1)t_t^2) - t_t(r_t^2 r_t^1 t_s^2 + r_s^2 r_t^1 t_t^2))\frac{\partial \mathbf{\Omega}_1}{\partial x} dx + i(t_s(r_t^2 r_t^1 t_s^2 + r_s^2 r_t^1 t_t^2) + t_t(r_t^2 r_s^1 t_s^2 + (1 + r_s^2 r_s^1)t_t^2))\mathbf{\Omega}_1 \times \frac{\partial \mathbf{\Omega}_1}{\partial x} dx$
$b_3 \boldsymbol{v}_3$	=	$(r_t + t_s(r_t^2 t_s + r_s^2 t_t) + t_t(r_s^2 t_s + r_t^2 t_t))\mathbf{\Omega}_1 + i(t_s r_t^2 t_t + t_t r_t^2 t_s)\mathbf{\Omega}_1 \times \frac{\partial \mathbf{\Omega}_1}{\partial x} dx + (t_s r_t^2 t_s - t_t r_t^2 t_t)\frac{\partial \mathbf{\Omega}_1}{\partial x} dx$

Table 1: The coefficients from Eq. (20) for all three terminals

2.2 A spin-current-induced charge current

So far we have considered a charge current on a FM-NM interface with non-constant magnetization that induces a transverse spin current into the normal metal. There is also a reverse effect, e.g. a charge current on the interface as a result of a spin current in the normal metal. To describe this, the theory of Onsager reciprocity will be used.

2.2.1 Onsager reciprocity

The first law of thermodynamics relates the entropy $\mathcal{S}$ to so-called state variables, like the energy U, the volume V and the number of particles N:

$$T d\mathcal{S} = dU + P dV - \mu dN. \tag{22}$$

In principle there can be more state variables, like the volume or the number of particles of another species. For every state variable a_i, we can define a conjugate force by

$$X_i = T \frac{\partial \mathcal{S}}{\partial a_i}. \tag{23}$$

For instance, the conjugate force of N is minus the chemical potential μ. In so called linear response, which ignores higher order contributions of the conjugate forces, we can write for the time derivative of every state variable a_i [10]

$$\dot{a_i} = \sum_{k=1}^{M} L_{ik} X_k. \tag{24}$$

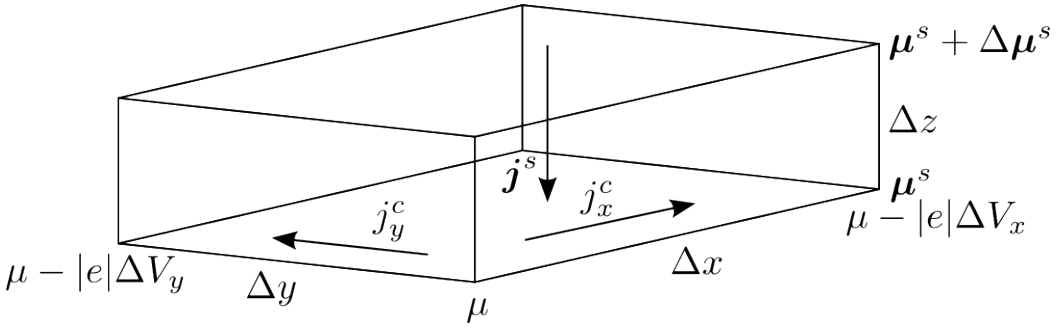

Figure 5: A small box on the NM-FM interface, with a spin current flowing in the z-direction and a charge current in the x- and y-direction. At the sides of the box the corresponding values of the (spin) chemical potential are given.

Here M is the number of state variables and L is some $M \times M$-matrix. The principle of Onsager reciprocity says there is a relation between the matrix coefficients which is given by [10]

$$L_{ik}(B_{ext}, \boldsymbol{\Omega}) = \epsilon_k \epsilon_i L_{ki}(-B_{ext}, -\boldsymbol{\Omega}), \tag{25}$$

where B_{ext} is an external magnetic field and $\boldsymbol{\Omega}$ is the unit magnetization in the system. The factor ϵ_i is 1 if the state variable is even under time reversal symmetry and -1 in any other case. For example, the velocity of a particle is odd under time reversal symmetry, because if the time is reversed the velocity of the particle will be in the opposite direction.

2.2.2 A spin-current-induced charge current

Now we return to the FM-NM interface. We consider a small box on the interface with dimensions Δx, Δy and Δz and a charge current flowing in the (x, y)-plane and a spin current in the negative z-direction. This implies the chemical potential decreases from μ to $\mu - |e|\Delta V_i$ in both directions i with the direction of the current. Similarly the value of the spin chemical potential, which is called the spin accumulation $\boldsymbol{\mu}^s$, is $\Delta\boldsymbol{\mu}^s$ higher on top of the small box. The situation is shown in Fig. 5.

In this case the only relevant state variables are N and $\boldsymbol{N}^s$, where the latter is the number of particles with spin in each direction. The volume of the box is kept fixed and we assume the total energy to be constant. The time derivative of (22) then reads

$$T\dot{\mathcal{S}} = -\mu\frac{dN}{dt} - \boldsymbol{\mu}^s \cdot \frac{d\boldsymbol{N}^s}{dt}. \tag{26}$$

If we consider the total change in the entropy of the box, the value for the sides where a current flows out needs to be subtracted from the value of the sides where the current flows in. We then find

$$T\dot{\mathcal{S}} = -|e|\Delta V_x\frac{dN_x}{dt} - |e|\Delta V_y\frac{dN_y}{dt} - \Delta\boldsymbol{\mu}^s \cdot \frac{d\boldsymbol{N}^s}{dt}. \tag{27}$$

Now we can make certain identifications: $|e|\frac{dN_i}{dt} = I_i$, the charge current in the i-direction, and $\frac{d\boldsymbol{N}^s}{dt} = \frac{2}{\hbar}\boldsymbol{I}^s$, with $\boldsymbol{I}^s$ the spin current. After dividing by the volume of the box $\Delta x\Delta y\Delta z$ and

taking the limit that the dimensions of the boxes go to zero, the intensive equation

$$T\dot{s} = \boldsymbol{E} \cdot \boldsymbol{j}^c - \frac{2|e|}{\hbar} \frac{\partial \boldsymbol{\mu^s}}{\partial z} \cdot \boldsymbol{j}^s, \tag{28}$$

arises, with $s = \frac{\mathcal{S}}{\Delta x \Delta y \Delta z}$ the entropy density, $\boldsymbol{E} = -\left(\frac{\Delta V_x}{\Delta x}, \frac{\Delta V_y}{\Delta y}\right)$ the electric field, $\boldsymbol{j}^c = \left(\frac{I_x}{\Delta y \Delta z}, \frac{I_y}{\Delta x \Delta z}\right)$ the charge current density and $\boldsymbol{j^s} = \frac{\boldsymbol{I}^s}{\Delta x \Delta y}$ the spin current density. Now, the principle of Onsager reciprocity comes into play. It states there exists a matrix L with the symmetry of Eq. (25) such that

$$\begin{pmatrix} j_i^c \\ j_j^s \end{pmatrix} = L \begin{pmatrix} E_i \\ -\frac{2}{\hbar} \frac{\partial \mu_j^s}{\partial z} \end{pmatrix}. \tag{29}$$

Using Ohm's law ($\boldsymbol{j}^c = \sigma \boldsymbol{E}$) in combination with Eq. (1) leads to an expression for L_{12}. Since a charge current is even under time reversal symmetry and a spin current is odd and the unit magnetization appears twice in Eq. (1), the only difference between the off diagonal terms of L is a minus sign, according to Eq. (25). The coefficient L_{12} relates the induced charge current to the gradient of the spin accumulation. To find the connection with the spin current density, a variant of Ohm's law for spin currents is needed: $\boldsymbol{j^s} = -\frac{\pi \hbar \sigma}{e^2} \frac{\partial \boldsymbol{\mu^s}}{\partial z}$ [4]. Rearranging terms gives

$$j_i^c = \frac{g g_L \mu_B P}{4\pi M_s |e|} \left(\boldsymbol{\Omega} \times \frac{\partial \boldsymbol{\Omega}}{\partial x_i} \right) \cdot \boldsymbol{j}^s, \tag{30}$$

which is the desired formula for a spin-current-induced charge current on the interface. For a spin current induced by the spin Hall effect, the spin current density is of order 10^{-6} kg s^{-1}, which implies, taking $\frac{\partial \boldsymbol{\Omega}}{\partial x_i} \approx \frac{1}{\lambda_{sk}} = 10^8$ m^{-1}, $g_L = 1.2$, $P = 0.40$, $g = 10^{15}$ Ω^{-1} m^{-2} and $M_s \approx 10^6$ A m^{-1}, an induced charge current density of order 10^4 A m^{-2}. Here λ_{sk} is the approximate skyrmion size, which is a length scale for the magnetization gradient, as we will see later on. This corresponds to a voltage difference ΔV of $\frac{\Delta V}{\lambda_{sk}} \approx 10^{-3}$ V m^{-1}, where we used $\sigma = 10^7$ Ω^{-1} m^{-1} for the conductivity. This voltage is small, but measurable.

3 Skyrmions on a FM-NM interface

Having discussed the spin current injection into a normal metal, we now turn to an application in the form of the dynamics of a skyrmion. A skyrmion is a spiral-like configuration of the magnetization, of which the movement is influenced by various torques including one as a result of a spin current. This torque is present because the injected spin current reduces the angular momentum of the skyrmion [4]. Because the presence of a skyrmion ensures that the magnetization is non-constant, a current through a FM-NM interface with a skyrmion will induce a spin current in the normal metal which in turn will influence the dynamics of the skyrmion. First we take a look at the skyrmion profile and after that we study the influence of the injected spin current on the dynamics of the skyrmion.

3.1 Skyrmion profile

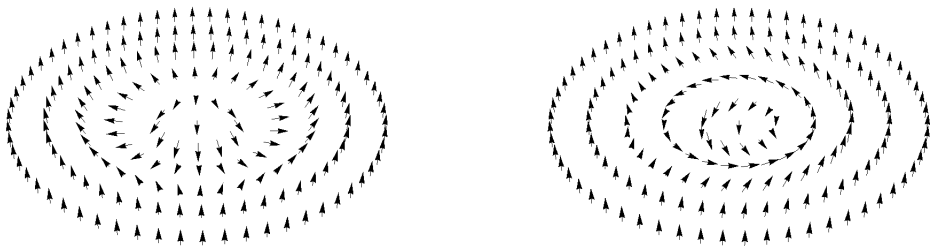

(a) $\phi_0 = 0$ (b) $\phi_0 = \pi/2$

Figure 6: A schematic picture of two skyrmions, with different azimuthal angle ϕ_0.

We consider a two dimensional FM-NM interface with a single skyrmion located on the interface. A skyrmion is a rotationally symmetric profile of the magnetization, such as shown in Fig. 6. After parameterizing the unit magnetization as $\mathbf{\Omega}(\boldsymbol{x}) = (\sin(\theta(\rho))\cos(\phi(\rho)), \sin(\theta(\rho))\sin(\phi(\rho))), \cos(\theta(\rho)))$ in terms of polar coordinates (ρ, φ), this symmetry is made explicit by making the functions θ and ϕ independent of the angle φ. Furthermore, the skyrmions we consider have constant azimuthal angle $\phi(\rho) = \phi_0$. The configuration of the skyrmion is determined by the energy functional $E(\mathbf{\Omega})$, as derived in Ref. [6]:

$$E(\mathbf{\Omega}) = d_F \int d\boldsymbol{x} \Big(-\frac{J_s}{2}\mathbf{\Omega}\cdot\nabla^2\mathbf{\Omega} + K(1-\Omega_z^2) + \frac{C}{2}(\hat{\boldsymbol{z}}\times\mathbf{\Omega})\cdot(\nabla\times\mathbf{\Omega}) + \mu_0 M_s H(1-\Omega_z) - \mu_0 M \mathbf{\Omega}\cdot\boldsymbol{H}_d \Big). \tag{31}$$

Here, d_F is the thickness of the ferromagnetic layer. The first term in Eq. (31) is proportional to the spin stiffness J_s and is an energy exchange term, which penalizes spatial changes in the magnetization. The second term, proportional to some constant K, is an anisotropy term, because the z-direction is favorable for the magnetization. The next term is the so called Dzyaloshinskii-Moriya interaction term and the last two terms correspond to an external magnetic field $H\hat{\boldsymbol{z}}$ and a dipolar field $\boldsymbol{H}_d$ respectively. To find the differential equation that determines the skyrmion

profile, one should plug in the parametrization of the magnetization and take the functional derivative to θ, just as in Ref. [6]. One then finds that θ obeys

$$\frac{d^2\theta}{d\tilde{\rho}} + \frac{1}{\tilde{\rho}}\frac{d\theta}{d\tilde{\rho}} - \frac{\sin\theta\cos\theta}{\tilde{\rho}^2} + \cos\phi_0\frac{\sin^2\theta}{\tilde{\rho}} - \left(C_1 + C_3\cos^2\phi_0\right)\sin\theta\cos\theta - C_2\sin\theta = 0. \quad (32)$$

Here, $C_1 = 2J_sK/C^2$, $C_2 = \mu_0 J_s HM/C^2$ and $C_3 = 2\mu_0 J_s M^2/C^2$ are all dimensionless constants and $\tilde{\rho} = \rho/\lambda_{sk}$ the dimensionless radial position, where $\lambda_{sk} = J_s/C$ is the approximate skyrmion size. It turns out that $C_1 \approx 16$, $C_2 \approx 0.36$, $C_3 \approx 9$ and $\phi_0 \approx 0$ [11]. By taking these values and using the boundary conditions $\theta(0) = \pi$ and $\theta(\infty) = 0$ we can numerically solve Eq. (32) for θ, which will be needed later on.

Now we return to the spin current injection from Eq. (1). After using the numerical solution found for the skyrmion profile, we can find the polarization and the strength of the spin current in the normal metal. Fig. 7(a) shows the direction of the spin polarization as a function of the position. In Fig. 7(b) the same plot is made for the situation with azimuthal angle $\phi_0 = \pi/2$, using the same function for the polar angle $\theta(\rho)$, which does not really depend on the azimuthal angle ϕ_0. It turns out that the spin polarization of the injected spin current strongly depends on the azimuthal angle ϕ_0.

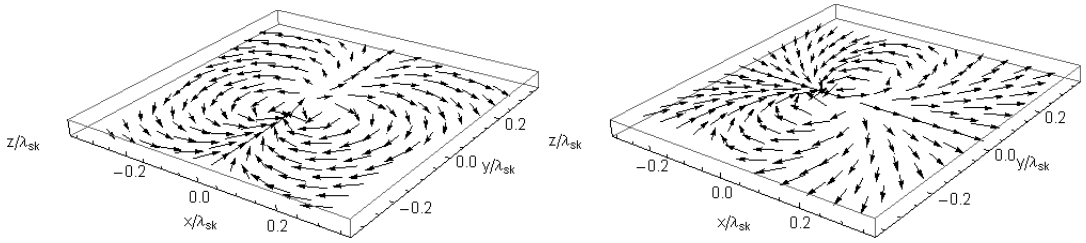

(a) $\phi_0 = 0$ (b) $\phi_0 = \pi/2$

Figure 7: The direction of the spin polarization as a function of the scaled position for two different angles of the azimuthal angle ϕ_0 of the skyrmion.

The magnitude of the spin current largely depends on the magnetization gradient of the skyrmion. Indeed, for the experimentally determined values in the previous paragraph, the gradient of θ is plotted in Fig. 8 for $\lambda_{sk} = 20$ nm. Since the injected spin current contains two terms, one containing the derivative of θ and one scaling with $\lambda_{sk}/\tilde{\rho}$, the injected spin current is negligible outside a small area, which is approximately a circle with radius λ_{sk}.

3.2 Dynamics of the skyrmion

As a result of the injected spin current in the normal metal, there is an additional torque that works on the skyrmion. Therefore, the presence of a non-magnetic layer will influence the dynamics of the skyrmion when a current flows trough the interface. First, we need the total spin current in the normal metal. As a result of the injected spin current, there will be spin accumulating at the interface, so the so-called spin accumulation $\boldsymbol{\mu}^s$ will be nonzero on the interface. As a result of this there will be a spin backflow in the normal metal. To find the backflow we first need the spin accumulation which obeys the spin diffusion equation [4]

$$\nabla^2\boldsymbol{\mu}^s(x,y,z) = \frac{\boldsymbol{\mu}^s(x,y,z)}{\lambda_{sd}^2}. \quad (33)$$

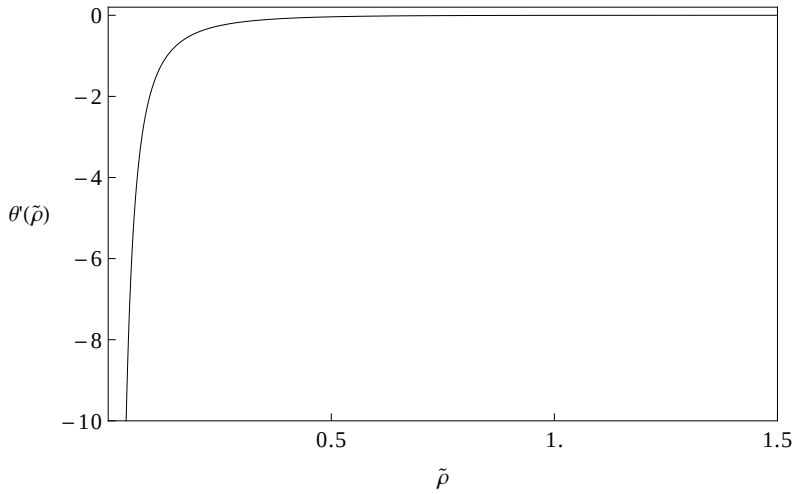

Figure 8: The derivative of θ as a function of $\tilde{\rho}$ for $\lambda_{sk} = 20$ nm.

Here, λ_{sd} is the spin diffusion length of the normal metal. Under the assumption the diffusion in the x- and y-direction is negligible, an analytical solution for the total spin flow can be obtained. This approximation is valid if the skyrmion size is much larger than the spin diffusion length of the normal metal. The solution for the spin accumulation is derived in Appendix A.3 and given by

$$\boldsymbol{\mu}^s = -\frac{4\pi\lambda_{sd}G_0\cosh\left(\frac{z+d_N}{\lambda_{sd}}\right)}{4\pi\sigma\sinh\left(\frac{d_N}{\lambda_{sd}}\right)+\lambda_{sd}g^{\uparrow\downarrow}\cosh\left(\frac{d_N}{\lambda_{sd}}\right)}\boldsymbol{j}^s_{in}. \tag{34}$$

Here, σ is the conductivity of the normal metal and d_N the thickness of the normal metal. Now, the backflow on the interface is proportional to the spin accumulation on the interface and the net flow on the interface, which is the sum of the inflow and the backflow, can be written as

$$\boldsymbol{j}^s_{net} = \frac{1}{1+\frac{\lambda_{sd}g^{\uparrow\downarrow}}{4\pi\sigma}\coth(\frac{d_N}{\lambda_{sd}})}\boldsymbol{j}^s_{\text{in}}. \tag{35}$$

Here $g^{\uparrow\downarrow}$ is the mixing conductance of the normal metal. The net spin flow induces an additional torque on the skyrmion, which is proportional to the net spin flow itself. In the presence of other torques as a result of the charge current, the dynamics of the skyrmion is described by the Landau-Lifschitz-Gilbert (LLG) equation, which reads [4, 6]

$$\frac{\partial\boldsymbol{\Omega}}{\partial t} = \frac{\gamma}{M_s}\boldsymbol{\Omega}\times\frac{\delta E[\boldsymbol{\Omega}]}{\delta\boldsymbol{\Omega}} - \alpha_G\boldsymbol{\Omega}\times\frac{\partial\boldsymbol{\Omega}}{\partial t} + \frac{\gamma}{M_s d_F}\boldsymbol{j}_{\text{net}} + \left.\frac{\partial\boldsymbol{\Omega}}{\partial t}\right|_{\text{current}}. \tag{36}$$

Here, γ is the gyromagnetic ratio, $E(\boldsymbol{\Omega})$ the energy functional from Eq. (31), α_G the Gilbert damping constant and d_F the thickness of the ferromagnet. The last term in the above equation describes the current-induced torques on the skyrmion and is given by

$$\left.\frac{\partial\boldsymbol{\Omega}}{\partial t}\right|_{\text{current}} = a(\boldsymbol{j}^c\cdot\nabla)\boldsymbol{\Omega} + a'\boldsymbol{\Omega}\times(\boldsymbol{j}^c\cdot\nabla)\boldsymbol{\Omega} + b\boldsymbol{\Omega}\times(\boldsymbol{j}^c\times\hat{\boldsymbol{z}}) + b'\boldsymbol{\Omega}\times(\boldsymbol{\Omega}\times(\boldsymbol{j}^c\times\hat{\boldsymbol{z}})), \tag{37}$$

where a, a', b and b' are system parameters that cannot be calculated analytically, in general.

To further study the dynamics we need a modified version of the Thiele equation, which describes the dynamics of a skyrmion. Since we are looking for solutions that minimize the energy, the term containing the functional derivative of the energy is zero. Assuming that the solution of the LLG equation is of the form $\mathbf{\Omega}(\boldsymbol{x}-\boldsymbol{X}(t))$, where $\boldsymbol{X}(t)$ is the position of the center of the skyrmion at time t, the Thiele equation can be obtained from the LLG equation by first taking the cross product of the LLG equation with $\mathbf{\Omega}$, then taking the inner product with $\frac{\partial \mathbf{\Omega}}{\partial x_i}$ after which one integrates over the whole space. The result is the following equation

$$-\epsilon_{ij}(\dot{X}_j + a j_j^c) = -D(\alpha_G \dot{X}_i + (a' + c') j_i^c) - b' \lambda_{sk} I' R_{ij} j_j^c, \tag{38}$$

as is derived in Appendix A.4. Here $c' = -\frac{\gamma g g_L \hbar \mu_B P}{2M_s^2 |e| d_F} \frac{1}{4\pi\sigma + \lambda_{sd} g^{\uparrow\downarrow} \coth(d_N/\lambda_{sd})}$ and D and I' are both dimensionless numbers, which can be calculated numerically for any skyrmion profile. Furthermore, R_{ij} is the 2×2 rotation matrix corresponding to a counterclockwise rotation over an angle ϕ_0. One of the current induced torques does not contribute to the velocity of the single skyrmion at all, as a result of the symmetries of the skyrmion. Since c' influences the skyrmion velocity in exactly the same way as a', it may seem to be possible to define a new constant which captures both contributions. However, this is not the case, since a' depends on the strength of a charge current-induced torque, while c' describes the torque on the skyrmion as a result of the spin injection into the normal metal, for which the normal metal needs to be present.
Since c' is negative, the presence of a normal metal layer slows the skyrmion down. The ratio between a' and c' is given by

$$\frac{c'}{a'} = -\frac{\gamma g \hbar}{M_s d_F \beta_0} \frac{1}{4\pi\sigma + \lambda_{sd} g^{\uparrow\downarrow} \coth(d_N/\lambda_{sd})}, \tag{39}$$

where β_0 is the nonadiabaticity parameter. Typical values for these parameters are $g = 10^{15}\ \Omega^{-1}$ m^{-2} $M_s = 3 \times 10^5$ A m^{-1}, $d_F = 3$ nm, $\beta_0 = 0.04$, $\sigma = 9.5 \times 10^6, \Omega^{-1}$ m^{-1}, $g^{\uparrow\downarrow} = 10^{15}\ \Omega^{-1}$ m^{-2}. In figure the ratio between the two coefficients is plotted as a function of the scaled thickness of the thickness of the normal metal $\frac{d_N}{\lambda_{sd}}$ for different values of the spin diffusion length λ_{sd}, where we have taken $\lambda_{sk} = 20$ nm.

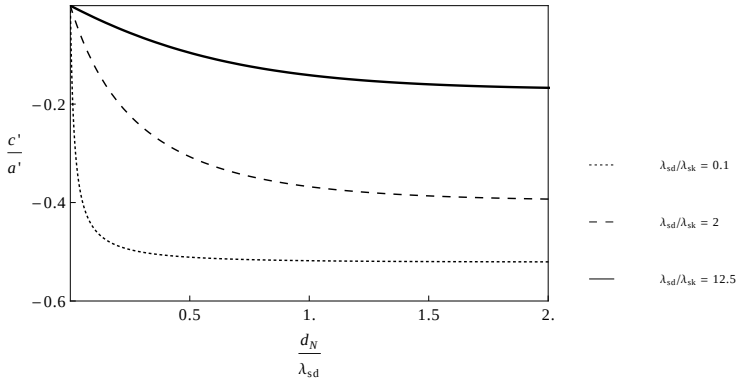

Figure 9: The ratio of c' and a' plotted as a function of the scaled thickness of the normal metal layer for different values of the spin diffusion length.

From Fig. (9), we see that the effect of the spin current induced torques increases as a function of the thickness of the normal metal. For small values of the spin diffusion length, the ratio between the coefficients does not really depend on the thickness of the normal metal layer,

because for realistic values of the thickness the ratio is already at its minimal value. However, for instance in copper, with $\lambda_{sd} \approx 250$ nm, the thickness of the copper layer does influence the values of the ratio between the coefficients. It should be noted that for these values of λ_{sd} the earlier assumption $\lambda_{sd} \ll \lambda_{sk}$ is false. In realistic settings, the skyrmion moves only in one direction. The reason for this is that in for instance the y-direction, the skyrmion will reach the end of the layer at some point. In that case there will be an extra force on the skyrmion in the y-direction, such that the speed $\dot{Y}$ will be zero. Using the Thiele equation, we can now make an estimate of the speed in the x-direction. Using the values above and $b' = \frac{\hbar\gamma\theta_{SH}}{2|e|M_s d_F}$ [11], $\lambda_{sd} = 2$ nm, $\boldsymbol{j}^c = 10^{11}\hat{\boldsymbol{x}}$ A m^{-2}, $\alpha_G = 0.2$, $d_N = 20$ nm, $d_F = 20$ nm and $\theta_{SH} = 0.1$, leads to $\dot{X} \approx 10$ m s^{-1}.

4 Discussion and conclusions

In this Thesis we considered a model for spin current injection from a ferromagnetic into a normal metal, using a continuum scattering method with three terminals. It was found that the polarization of the spin current depends on the cross product of the magnetization and its gradient, which was derived in Ref. [4] using a completely different model. However, two other terms were also present. After that, a mechanism for the detection of a spin current was constructed, using the reverse effect of what we just described. For a spin current induced by the spin Hall effect, we found that the induced charge current leads to a voltage in the order of nanovolts, which is certainly measurable.

It should be noted that the injected spin current is first order in gradients of the magnetization. One can find a more accurate description if higher order terms are considered as well. Furthermore, the model assumes all terminals are small enough to be treated one-dimensionally, which means only the zeroth mode is occupied in the transverse direction. This could be improved by allowing higher modes in the transverse direction as well, which would lead to transmission and reflection coefficients that not only depend on the spin and wave number of the incoming wave, but on the transverse mode as well.

In the second model, with two magnetic regions, only terms with at most two reflections between those regions were considered. An analytical solution for the case with infinite reflections can be obtained using a geometric series. The injected spin current would still be a linear combination of the magnetization, its derivative and their cross product. However, the coefficients in front of those vectors would also depend on the magnetization.

In the future, one could use a more realistic model for the band structure in the metal. Now, we have assumed that all energies below the chemical potential are allowed. To give a more accurate description, the band structures of the metal can be taken into account. In that case, some energies are excluded from the integrals. It should be noted that in that case the injected spin current is still a linear combination of the same vectors, but the coefficients in front of them will, in general, be different.

In the second part, we found that the spin current injection can be used to tune the speed of a skyrmion on a FM-NM interface. Since one of the current induced torques is exactly of the same form as the spin current induced torque, one can measure the effect of the spin current on the skyrmion by varying the thickness of the normal metal layer, because the ratio of the strength of the two torques is of order unity for reasonable values of the thickness.

For skyrmions, the polarization of the injected spin currents is highly dependent on the constant azimuthal angle ϕ_0, which is an example of the fact that the polarization can change drastically if the magnetization is changed, which follows from Eq. (1). Since for a skyrmion the magnetization is practically constant outside a region with sides of the order of 10 nm, the spin current is injected only locally into the normal metal.

The torque on the skyrmion was derived, assuming that the injected spin current diffuses only in the z-direction. This assumption is valid if the skyrmion size is much larger than the spin diffusion length, which is not always true for realistic situations. When diffusion in the other direction is included, one has to resort to numerical methods to find a solution of the spin diffusion equation (33). One way to do this, is rewriting the differential equation Eq. (33) into the integral equation [4]

$$\int dx' K(x - x', y - y', z) \boldsymbol{j}^s_{net}(x', y'), \tag{40}$$

and it can be shown that the Fourier transform of the kernel $K(k_x, k_y, z)$ of this integral equation

is equal to

$$\hat{K}(k_x, k_y, z) = -\frac{G_0 \lambda_{sd}}{\sigma} \frac{\cosh(\frac{z+d_N}{\lambda_{sd}} \sqrt{(k_x^2 + k_y^2)\lambda_{sd}^2 + 1})}{\sqrt{(k_x^2 + k_y^2)\lambda_{sd}^2 + 1} \sinh(\frac{d_N}{\lambda_{sd}} \sqrt{(k_x^2 + k_y^2)\lambda_{sd}^2 + 1})}. \tag{41}$$

However, the backflow term in the net spin current $\boldsymbol{j}_{net}^s$ depends on $\boldsymbol{\mu}^s$ itself and to find an actual solution an iterative method could be used.

A possible direction for future research is a lattice of skyrmions instead of only a single skyrmion. In that case, the skyrmions will also interact with each other, leading to extra torques that should be considered, which will influence their motion.

A Appendix

A.1 Derivation of the transmitted spin current

We start from Eq. (4) which is

$$\boldsymbol{I}^s_{1,1,\uparrow} = -\frac{\hbar^2 k}{2m}\left(t^*_{\uparrow\uparrow}\langle\uparrow| + t^*_{\uparrow\downarrow}\langle\downarrow|\right)\boldsymbol{\tau}\left(t_{\uparrow\uparrow}\,|\uparrow\rangle + t_{\uparrow\downarrow}\,|\downarrow\rangle\right). \tag{42}$$

Now, we can simplify this using the expectation value for the Pauli matrices which are

$$\langle\uparrow|\,\boldsymbol{\tau}\,|\uparrow\rangle = -\langle\downarrow|\,\boldsymbol{\tau}\,|\downarrow\rangle = \hat{\boldsymbol{z}}; \tag{43a}$$

$$\langle\uparrow|\,\boldsymbol{\tau}\,|\downarrow\rangle = (\langle\downarrow|\,\boldsymbol{\tau}\,|\downarrow\rangle)^* = \hat{\boldsymbol{x}} - i\hat{\boldsymbol{y}}, \tag{43b}$$

and plug this in to find:

$$\begin{aligned} I^s_{1,1\uparrow,x} &= -\frac{\hbar^2 k}{2m}(t^*_{\uparrow\uparrow}t_{\uparrow\downarrow} + t_{\uparrow\uparrow}t^*_{\uparrow\downarrow}) \\ &= -\frac{\hbar^2 k}{2m}((t^*_s + t^*_t\Omega_z)t_t(\Omega_x + i\Omega_y) + (t_s + t_t\Omega_z)t^*_t(\Omega_x - i\Omega_y)) \\ &= -\frac{\hbar^2 k}{2m}((t^*_s t_t + t_s t^*_t)\Omega_x + 2|t_t|^2\Omega_z\Omega_x + i(t^*_s t_t - t_s t^*_t)\Omega_y), \end{aligned} \tag{44}$$

and

$$\begin{aligned} I^s_{1,1\uparrow,y} &= -\frac{i\hbar^2 k}{2m}(-t^*_{\uparrow\uparrow}t_{\uparrow\downarrow} + t_{\uparrow\uparrow}t^*_{\uparrow\downarrow}) \\ &= -\frac{i\hbar^2 k}{2m}(-(t^*_s + t^*_t\Omega_z)t_t(\Omega_x + i\Omega_y) + (t_s + t_t\Omega_z)t^*_t(\Omega_x - i\Omega_y)) \\ &= -\frac{\hbar^2 k}{2m}(-i(t^*_s t_t - t_s t^*_t)\Omega_x - 2i|t_t|^2\Omega_z\Omega_y + (t^*_s t_t + t_s t^*_t)\Omega_y), \end{aligned} \tag{45}$$

and

$$\begin{aligned} I^s_{1,1\uparrow,z} &= -\frac{\hbar^2 k}{2m}(|t_{\uparrow\uparrow}|^2 - |t_{\uparrow\downarrow}|^2) \\ &= -\frac{\hbar^2 k}{2m}((t^*_s + t^*_t\Omega_z)(t_s + t_t\Omega_z) - t^*_t(\Omega_x - i\Omega_y)t_t(\Omega_x + i\Omega_y)) \\ &= -\frac{\hbar^2 k}{2m}(|t_s|^2 + (t^*_s t_t + t_s t_t*)\Omega_z + |t_t|^2\Omega_z^2 - |t_t|^2(\Omega_x^2 + \Omega_y^2)) \\ &= -\frac{\hbar^2 k}{2m}(|t_s|^2 + |t_t|^2(2\Omega_z - 1) + (t^*_s t_t + t_s t^*_t)\Omega_z). \end{aligned} \tag{46}$$

We can do a similar thing for an electron with spin $|\downarrow\rangle$:

$$\boldsymbol{I}^s_{1,1\downarrow} = -\frac{\hbar^2 k}{2m}\left(t^*_{\downarrow\downarrow}\langle\downarrow| + t^*_{\downarrow\uparrow}\langle\uparrow|\right)\boldsymbol{\tau}\left(t_{\downarrow\downarrow}\,|\downarrow\rangle + t_{\downarrow\uparrow}\,|\uparrow\rangle\right). \tag{47}$$

Simplifying leads to

$$\begin{aligned} I^s_{1,1\downarrow,x} &= -\frac{\hbar^2 k}{2m}(t^*_{\downarrow\downarrow}t_{\downarrow\uparrow} + t_{\downarrow\downarrow}t^*_{\downarrow\uparrow}) \\ &= -\frac{\hbar^2 k}{2m}((t^*_s - t^*_t\Omega_z)t_t(\Omega_x - i\Omega_y) + (t_s - t_t\Omega_z)t^*_t(\Omega_x + i\Omega_y)) \\ &= -\frac{\hbar^2 k}{2m}((t^*_s t_t + t_s t^*_t)\Omega_x - 2|t_t|^2\Omega_z\Omega_x + i(-t^*_s t_t + t_s t^*_t)\Omega_y), \end{aligned} \tag{48}$$

and

$$\begin{aligned} I^s_{1,1\downarrow,y} &= -\frac{i\hbar^2 k}{2m}(t^*_{\downarrow\downarrow}t_{\downarrow\uparrow} - t_{\downarrow\downarrow}t^*_{\downarrow\uparrow}) \\ &= -\frac{i\hbar^2 k}{2m}((t^*_s - t^*_t\Omega_z)t_t(\Omega_x - i\Omega_y) - (t_s - t_t\Omega_z)t^*_t(\Omega_x + i\Omega_y)) \\ &= -\frac{\hbar^2 k}{2m}(i(t^*_s t_t - t_s t^*_t)\Omega_x + 2i|t_t|^2\Omega_z\Omega_y + (t^*_s t_t + t_s t^*_t)\Omega_y), \end{aligned} \tag{49}$$

and

$$\begin{aligned} I^s_{1,1\downarrow,z} &= -\frac{\hbar^2 k}{2m}(-|t_{\downarrow\downarrow}|^2 + |t_{\downarrow\uparrow}|^2) \\ &= -\frac{\hbar^2 k}{2m}(-(t^*_s - t^*_t\Omega_z)(t_s - t_t\Omega_z) + t^*_t(\Omega_x + i\Omega_y)t_t(\Omega_x - i\Omega_y)) \\ &= -\frac{\hbar^2 k}{2m}(-|t_s|^2 + (t^*_s t_t + t_s t_t*)\Omega_z - |t_t|^2\Omega_z^2 + |t_t|^2(\Omega_x^2 + \Omega_y^2)) \\ &= -\frac{\hbar^2 k}{2m}(|t_s|^2 - |t_t|^2(2\Omega_z - 1) + (t^*_s t_t + t_s t^*_t)\Omega_z). \end{aligned} \tag{50}$$

To find the spin current in terminal 3 as a result of electrons entering terminal 1, we sum the contributions of the spin $|\uparrow\rangle$ and spin $|\downarrow\rangle$ electrons, to find

$$\boldsymbol{I}^s_{1,1\uparrow} + \boldsymbol{I}^s_{1,1\downarrow} = -\frac{\hbar^2 k}{m}(t^*_s t_t + t_s t^*_t)\boldsymbol{\Omega}. \tag{51}$$

Integrating this over all possible values of k leads to Eq. (5). Similar expression hold for the contributions of terminal 2 and 3. For terminal 3, the wave function is slightly different and is given by

$$\psi(y) = Ae^{iky}\,|\uparrow\rangle + Ae^{-iky}((r_{\uparrow\uparrow})\,|\uparrow\rangle + r_{\uparrow\downarrow}\,|\downarrow\rangle)\,, \tag{52}$$

for a particle incoming with spin $|\uparrow\rangle$. However, the extra term cancels when one adds the contribution of the spin down particles. Intuitively, this is clear, because for the incoming particles in terminal 3 there is no preferred direction for the spin, so they will not contribute to the spin current.

A.2 Transmission and reflection coefficients

In this appendix we find explicit expressions for the a_i, b_i and $\boldsymbol{v}_i$ in Eq. (20). We start with the case $i = 1$. Using (21), we calculate

$$\begin{aligned} t_{1\to 3} &= t + tr^2t^1 = t + t((r^2_s t^1_s + r^2_t t^1_t)\mathbb{1} + (r^2_t t^1_s\boldsymbol{\Omega}_2 + r^2_t t^1_s\boldsymbol{\Omega}_1 + ir^2_t t^1_t\boldsymbol{\Omega}_1 \times \boldsymbol{\Omega}_2)\cdot\boldsymbol{\tau}) \\ &= (t_s(1 + r^2_s t^1_s + r^2_t t^1_t) + t_t(r^2_t t^1_s + r^2_s t^1_t))\mathbb{1} + ((t_s(r^2_t t^1_s + r^2_s t^1_t) + t_t(1 + r^2_s t^1_s + r^2_t t^1_t))\boldsymbol{\Omega}_1 \\ &+ i(t_s r^2_t t^1_t + t_t r^2_t t^1_s)\boldsymbol{\Omega}_1 \times \frac{\partial\boldsymbol{\Omega}_1}{\partial x}dx + (t_s r^2_t t^1_s - t_t r^2_t t^1_t)\frac{\partial\boldsymbol{\Omega}_1}{\partial x}dx)\cdot\boldsymbol{\tau}, \end{aligned} \tag{53}$$

where we used $\mathbf{\Omega}_2 = \mathbf{\Omega}_1 + \frac{\partial \mathbf{\Omega}_1}{\partial x} dx$ and $\mathbf{\Omega}_1 \cdot \frac{\partial \mathbf{\Omega}_1}{\partial x} dx = 0$, which follows from the fact that $\mathbf{\Omega}$ is a unit vector. For $i = 2$ we find

$$\begin{aligned}
t_{2\to 3} &= t(\mathbb{1} + r^2 r^1) t^2 \\
&= (t_s((1 + r_s^2 r_s^1 + r_t^2 r_t^1) t_s^2 + (r_s^2 r_t^1 + r_t^2 r_s^1)) t_t^2 + t_t((1 + r_s^2 r_s^1 + r_t^2 r_t^1) t_t^2 \\
&+ (r_s^2 r_t^1 + r_t^2 r_s^1) t_s^2)) \mathbb{1} + ((t_s((1 + r_s^2 r_s^1 + r_t^2 r_t^1) t_s^2 + (r_s^2 r_t^1 + r_t^2 r_s^1)) t_t^2 \\
&+ t_t((1 + r_s^2 r_s^1 + r_t^2 r_t^1) t_t^2 + (r_s^2 r_t^1 + r_t^2 r_s^1) t_s^2)) \mathbf{\Omega}_1 \\
&+ (t_s(r_t^2 r_s^1 t_s^2 + (1 + r_s^2 r_s^1) t_t^2) - t_t(r_t^2 r_t^1 t_s^2 + r_s^2 r_t^1 t_t^2)) \frac{\partial \mathbf{\Omega}_1}{\partial x} dx \\
&+ i(t_s(r_t^2 r_t^1 t_s^2 + r_s^2 r_t^1 t_t^2) + t_t(r_t^2 r_s^1 t_s^2 + (1 + r_s^2 r_s^1) t_t^2)) \mathbf{\Omega}_1 \times \frac{\partial \mathbf{\Omega}_1}{\partial x} dx) \cdot \boldsymbol{\tau},
\end{aligned} \tag{54}$$

and for $i = 3$ we have

$$\begin{aligned}
t_{3\to 3} = r + t r^2 t &= (r_s + t_s(r_s^2 t_s + r_t^2 t_t) + t_t(r_t^2 t_s + r_s^2 t_t)) \mathbb{1} + ((r_t + t_s(r_t^2 t_s + r_s^2 t_t) \\
&+ t_t(r_s^2 t_s + r_t^2 t_t)) \mathbf{\Omega}_1 + i(t_s r_t^2 t_t + t_t r_t^2 t_s) \mathbf{\Omega}_1 \times \frac{\partial \mathbf{\Omega}_1}{\partial x} dx + (t_s r_t^2 t_s - t_t r_t^2 t_t) \frac{\partial \mathbf{\Omega}_1}{\partial x} dx) \cdot \boldsymbol{\tau}.
\end{aligned} \tag{55}$$

Now, we have written all complete transmission and reflection coefficients in the desired form.

A.3 Approximate solution to the spin diffusion equation

In this appendix we derive Eq. (34) from Eq. (33) using the approximation that $\nabla^2 = \frac{\partial^2}{\partial z^2}$. First we need the boundary conditions for this differential equation:

$$\left. \frac{\partial \boldsymbol{\mu}}{\partial z} \right|_{z=-d_N} = 0; \tag{56a}$$

$$\left. \frac{\partial \boldsymbol{\mu}}{\partial z} \right|_{z=0} = -\frac{G_0}{\sigma} (\boldsymbol{j}_{in}^s + \boldsymbol{j}_{back}^s). \tag{56b}$$

These equations say that the gradient of the spin accumulation should scale with the spin current on the boundary of the normal metal. The backflow $\boldsymbol{j}_{back}^s$ on the interface scales with the spin accumulation itself

$$\boldsymbol{j}_{back}^s = \frac{g^{\uparrow\downarrow}}{4\pi G_0} \boldsymbol{\mu} \Big|_{z=0}. \tag{57}$$

To find the solution to these set of equations, we use the ansatz $\boldsymbol{\mu}(x, y, z) = \boldsymbol{f}(x, y) \cosh(z/\lambda_{sd} + z_0)$ with $\boldsymbol{f}$ an arbitrary vector valued function and z_0 some real number. This leads to

$$\boldsymbol{\mu} = -\frac{4\pi \lambda_{sd} G_0 \cosh(\frac{z + d_N}{\lambda_{sd}})}{4\pi\sigma \sinh(\frac{d_N}{\lambda_{sd}}) + \lambda_{sd} g^{\uparrow\downarrow} \cosh(\frac{d_N}{\lambda_{sd}})} \boldsymbol{j}_{in}^s. \tag{58}$$

We immediately find the backflow of the spin current, using equation (57) as

$$\boldsymbol{j}_{\text{back}}^s = -\frac{1}{\frac{4\pi\sigma}{\lambda_{sd} g^{\uparrow\downarrow}} \tanh(\frac{d_N}{\lambda_{sd}}) + 1} \boldsymbol{j}_{in}^s, \tag{59}$$

and the net spin spin flow, given by the sum of the injected spin current and the backflow, as

$$\boldsymbol{j}^s_{\text{net}} = \frac{1}{1+\frac{\lambda_{sd}g^{\uparrow\downarrow}}{4\pi\sigma}\text{cotanh}(\frac{d_N}{\lambda})}\boldsymbol{j}^s_{\text{in}}, \tag{60}$$

which is Eq. (34).

A.4 Derivation of the Thiele equation

The Thiele equation in Eq. (38) can be derived from Eq. (36), using the ansatz $\boldsymbol{\Omega}(\boldsymbol{x}-\boldsymbol{X}(t))$. To do this, we first take the cross product of $\boldsymbol{\Omega}$ with the LLG equation and subsequently take the inner product with $\frac{\partial\boldsymbol{\Omega}}{\partial x_i}$. The last step is integrating the resulting equation over the whole space. Now, we are going to follow these steps for all terms in the LLG equation. We are looking for solutions of the equations of motion and such solutions minimize the energy. Therefore, the term containing the functional derivative of the energy functional is zero in this description. For the first term $\frac{\partial\boldsymbol{\Omega}}{\partial t}$, we have

$$\int d\boldsymbol{x}\frac{\partial\boldsymbol{\Omega}}{\partial x_i}\cdot(\boldsymbol{\Omega}\times\frac{\partial\boldsymbol{\Omega}}{\partial t}) = \int d\boldsymbol{x}\frac{\partial\boldsymbol{\Omega}}{\partial x_i}\cdot(\boldsymbol{\Omega}\times(-\dot{X}_j\frac{\partial\boldsymbol{\Omega}}{\partial x_j})) = -\dot{X}_j\int d\boldsymbol{x}\;\boldsymbol{\Omega}\cdot\left(\frac{\partial\boldsymbol{\Omega}}{\partial x_j}\times\frac{\partial\boldsymbol{\Omega}}{\partial x_i}\right) = 4\pi\epsilon_{ij}\dot{X}_jW, \tag{61}$$

where W is the winding number of the skyrmion, defined by $W=\frac{1}{4\pi}\int \mathrm{d}\boldsymbol{x}\boldsymbol{\Omega}\cdot(\frac{\partial\boldsymbol{\Omega}}{\partial x}\times\frac{\partial\boldsymbol{\Omega}}{\partial y})$. The winding number of a skyrmion is always an integer and is in this case given by $W=-1$.
For the second term in the equation we first remark

$$\boldsymbol{\Omega}\times\left(\boldsymbol{\Omega}\times\frac{\partial\boldsymbol{\Omega}}{\partial t}\right) = \boldsymbol{\Omega}\left(\boldsymbol{\Omega}\cdot\frac{\partial\boldsymbol{\Omega}}{\partial t}\right) - \frac{\partial\boldsymbol{\Omega}}{\partial t}(\boldsymbol{\Omega}\cdot\boldsymbol{\Omega}) = -\frac{\partial\boldsymbol{\Omega}}{\partial t}, \tag{62}$$

where we have used the fact that $\boldsymbol{\Omega}$ is a unit vector, which implies $0=\frac{1}{2}\frac{\partial}{\partial t}||\boldsymbol{\Omega}|| = \boldsymbol{\Omega}\cdot\frac{\partial\boldsymbol{\Omega}}{\partial t}$. Using the descriptions of the derivatives $\frac{\partial}{\partial x}$ and $\frac{\partial}{\partial y}$ in cylindrical coordinates we find:

$$\frac{\partial\boldsymbol{\Omega}}{\partial x}\cdot\frac{\partial\boldsymbol{\Omega}}{\partial t} = -\left(\cos^2\varphi\left(\frac{d\theta}{d\rho}\right)+\frac{\sin^2\theta\sin^2\varphi}{\rho^2}\right)\dot{X}-\left(\sin\varphi\cos\varphi\left(\left(\frac{d\theta}{d\rho}\right)^2-\frac{\sin^2\theta}{\rho^2}\right)\right)\dot{Y} \tag{63}$$

$$\frac{\partial\boldsymbol{\Omega}}{\partial y}\cdot\frac{\partial\boldsymbol{\Omega}}{\partial t} = -\left(\sin^2\varphi\left(\frac{d\theta}{d\rho}\right)+\frac{\sin^2\theta\cos^2\varphi}{\rho^2}\right)\dot{Y}-\left(\sin\varphi\cos\varphi\left(\left(\frac{d\theta}{d\rho}\right)^2-\frac{\sin^2\theta}{\rho^2}\right)\right)\dot{X}. \tag{64}$$

So the desired integral is given by

$$\int d\boldsymbol{x}\frac{\partial\boldsymbol{\Omega}}{\partial x_i}\cdot\left(\boldsymbol{\Omega}\times\left(-\alpha_G\boldsymbol{\Omega}\times\frac{\partial\boldsymbol{\Omega}}{\partial t}\right)\right) = \alpha_G\int d\boldsymbol{x}\frac{\partial\boldsymbol{\Omega}}{\partial x_i}\cdot\frac{\partial\boldsymbol{\Omega}}{\partial t} = -4\pi\alpha_G D\dot{X}_i, \tag{65}$$

where D is a dimensionless number given by $D=\frac{1}{4}\int_0^\infty d\rho(\frac{\sin^2\theta}{\rho}+\rho(\frac{d\theta}{\mathrm{d}\rho})^2)$.
Now, we are ready to calculate the two current-induced torques that contain a gradient of the magnetization. Indeed, by writing

$$\frac{\partial\boldsymbol{\Omega}}{\partial t} = -(\dot{\boldsymbol{X}}\cdot\nabla)\boldsymbol{\Omega}, \tag{66}$$

we see that those terms are of the same form as the two terms we just calculated. Therefore, we have

$$\int d\boldsymbol{x} \frac{\partial \boldsymbol{\Omega}}{\partial x_i} \cdot (\boldsymbol{\Omega} \times a(\boldsymbol{j}^c \cdot \nabla)\boldsymbol{\Omega}) = -4\pi a \epsilon_{ij} j_j W; \tag{67}$$

$$\int d\boldsymbol{x} \frac{\partial \boldsymbol{\Omega}}{\partial x_i} \cdot (\boldsymbol{\Omega} \times a'(\boldsymbol{\Omega} \times (\boldsymbol{j}^c \cdot \nabla)\boldsymbol{\Omega})) = -4\pi a' \epsilon_{ij} j_j D. \tag{68}$$

For the next term we first note:

$$\frac{d\boldsymbol{\Omega}}{dx_i} \cdot (\boldsymbol{\Omega} \times (b\boldsymbol{\Omega} \times (\boldsymbol{j}^c \times \hat{\boldsymbol{z}}))) = b \frac{d\boldsymbol{\Omega}}{dx_i} \cdot (\boldsymbol{\Omega} \left(\boldsymbol{\Omega} \cdot (\boldsymbol{j}^c \times \hat{\boldsymbol{z}})\right) - \boldsymbol{j}^c \times \hat{\boldsymbol{z}} \left(\boldsymbol{\Omega} \cdot \boldsymbol{\Omega}\right)) = -b \left(\frac{d\boldsymbol{\Omega}}{dx_i} \cdot (\boldsymbol{j}^c \times \hat{\boldsymbol{z}}) \right). \tag{69}$$

The first term vanishes because the change in the unit vector $\boldsymbol{\Omega}$ is always perpendicular to the vector itself, as we saw earlier. We find, using polar coordinates and integrating the φ-coordinate,

$$\int d\boldsymbol{x} \frac{\partial \boldsymbol{\Omega}}{\partial x} \cdot (\boldsymbol{j}^c \times \hat{\boldsymbol{z}}) = 4\pi(-j_1^c \sin(\phi_0) + j_2^c \cos(\phi_0))\lambda_{sk} I; \tag{70}$$

$$\int d\boldsymbol{x} \frac{\partial \boldsymbol{\Omega}}{\partial y} \cdot (\boldsymbol{j}^c \times \hat{\boldsymbol{z}}) = 4\pi(-j_1^c \cos(\phi_0) - j_2^c \sin(\phi_0))\lambda_{sk} I. \tag{71}$$

In this equation, I is a dimensionless number, given by $I = \frac{1}{4}\int_0^\infty d\tilde{\rho}\, (\sin\theta + \tilde{\rho}\cos\theta \frac{d\theta}{d\tilde{\rho}})$, where we introduced the dimensionless variable $\tilde{\rho} = \frac{\rho}{\lambda_{sk}}$. By writing $\cos\theta \frac{d\theta}{d\tilde{\rho}} = \frac{d\sin\theta}{d\tilde{\rho}}$, we find $I = 0$ after partial integration. The boundary term at infinity vanishes since $\theta(\rho)$ goes faster to zero than $\frac{1}{\rho}$. (In fact, for the solutions of the differential equation that determines the skyrmion profiles, θ is practically zero if ρ is greater than a certain value which is approximately the skyrmion size λ_{sk}.)
For the last term we note that

$$\boldsymbol{\Omega} \times (\boldsymbol{\Omega} \times (\boldsymbol{\Omega} \times (\boldsymbol{j}^c \times \hat{\boldsymbol{z}}))) = -\boldsymbol{\Omega} \times (\boldsymbol{j}^c \times \hat{\boldsymbol{z}}) = \hat{\boldsymbol{z}}(\boldsymbol{\Omega} \cdot \boldsymbol{j}^c) - \boldsymbol{j}^c(\boldsymbol{\Omega} \cdot \hat{\boldsymbol{z}}). \tag{72}$$

For the desired integrals, we then find:

$$\int \mathrm{d}\boldsymbol{x} \left(\left(\frac{\partial \boldsymbol{\Omega}}{\partial x} \cdot \hat{\boldsymbol{z}} \right) (\boldsymbol{\Omega} \cdot \boldsymbol{j}^c) - \left(\frac{\partial \boldsymbol{\Omega}}{\partial x} \cdot \boldsymbol{j}^c \right) (\boldsymbol{\Omega} \cdot \hat{\boldsymbol{z}}) \right) = 4\pi(-j_1^c \cos(\phi_0) + j_2^c \sin(\phi_0))\lambda_{sk} I'; \tag{73}$$

$$\int \mathrm{d}\boldsymbol{x} \left(\left(\frac{\partial \boldsymbol{\Omega}}{\partial y} \cdot \hat{\boldsymbol{z}} \right) (\boldsymbol{\Omega} \cdot \boldsymbol{j}^c) - \left(\frac{\partial \boldsymbol{\Omega}}{\partial x} \cdot \boldsymbol{j}^c \right) (\boldsymbol{\Omega} \cdot \hat{\boldsymbol{z}}) \right) = 4\pi(-j_1^c \sin(\phi_0) - j_2^c \cos(\phi_0))\lambda_{sk} I'. \tag{74}$$

I' is another dimensionless number, given by an integral as well: $I' = \frac{1}{4}\int d\tilde{\rho}\, (\sin\theta\cos\theta - \theta)$. We can write the above equations in the following convenient way:

$$\int \mathrm{d}\boldsymbol{x} \frac{\partial \boldsymbol{\Omega}}{\partial x_i} \cdot (\boldsymbol{\Omega} \times (b'\boldsymbol{\Omega} \times (\boldsymbol{\Omega} \times (\boldsymbol{j}^c \times \hat{\boldsymbol{z}})))) = b'\lambda_{sk} I'_{ij} j_j^c, \tag{75}$$

where we introduced $I'_{ij} = -I' R_{ij}(\phi_0)$, with R_{ij} the elements of the orthogonal matrix corresponding to a counterclockwise rotation of the plane over an angle ϕ_0.

The only contribution to be included is the one of the net spin current on the interface. We note that, combining equation (1) and (60), that we can write

$$\frac{\gamma}{M_s d_F}\boldsymbol{j}^s_{\text{net}} = c'\boldsymbol{\Omega} \times (\boldsymbol{j}^c \cdot \nabla)\boldsymbol{\Omega}, \tag{76}$$

with $c' = -\frac{\gamma g g_L \hbar \mu_B P}{2M_s^2 |e| d_F} \frac{1}{4\pi\sigma + \lambda_{sd} g^{\uparrow\downarrow} \text{cotanh}(d_N/\lambda_{sd})}$. This is of exactly the same form as one of the current-induced torques, for which we earlier calculated the contribution. So collecting all the terms, we find the so called Thiele equation:

$$-\epsilon_{ij}(\dot{X}_j + a j^c_j) = -D(\alpha_G \dot{X}_i + (a' + c') j^c_i) + b' \lambda_{sk} I'_{ij} j^c_j. \tag{77}$$

References

[1] Wolf, S.A. "Spintronics: a Spin-Based Electronics Vision for the Future." *Science*. 294.5546 (2001): 1488-1495.

[2] Hirsch, J. "Spin Hall Effect." Physical Review Letters. 83.9 (1999): 1834-1837.

[3] Slachter, A, F.L. Bakker, J. Adam, and B.J. van Wees. "Thermally Driven Spin Injection from a Ferromagnet into a Non-Magnetic Metal." *Nature Physics*. 6.11 (2010): 879-882.

[4] Bijl, E. van der, R.E Troncoso, and R.A Duine. "Magnetic-texture-controlled Transverse Spin Injection." *Physical Review. B, Condensed Matter and Materials Physics*. 88.6 (2013): 64417.

[5] Fert, A., V. Cros, and J. Sampaio. "Skyrmions on the Track." *Nature Nanotechnology*. 8.3 (2013): 152-156.

[6] Knoester, M.E., J. Sinova, and R.A. Duine. "Phenomenology of Current-Skyrmion Interactions in Thin Films with Perpendicular Magnetic Anisotropy." *Physical Review. B, Condensed Matter and Materials Physics*. 89.6 (2014): 64425

[7] Datta, S., "Electronic Transport in Mesoscopic Systems." *Cambridge: Cambridge University Press*, 1995.

[8] Jiang, Y., X. Lu, F. Zhai. "Standard form of the scattering matrix for time reversal symmetric system" *arXiv:1310.3733 [cond-mat.mes-hall]*. (2013)

[9] Beenakker, C. "Random-matrix Theory of Quantum Transport." *Reviews of Modern Physics*. 69.3 (1997): 731-808.

[10] Bauer, G.E.W., S. Bretzel, A. Brataas, and Y. Tserkovnyak. "Nanoscale Magnetic Heat Pumps and Engines." *Physical Review. B, Condensed Matter and Materials Physics*. 81.2 (2010)

[11] Emori, S., U. Bauer, S. Ahn, E. Martinez, and G.S.D. Beach. "Current-driven Dynamics of Chiral Ferromagnetic Domain Walls." *Nature Materials*. 12.7 (2013): 611-616.